Continuous, Near-Bed Current Velocity Estimation Using Pressure and Inertial Sensing

Asko Ristolainen, Jeffrey A. Tuhtan ⓘD, and Maarja Kruusmaa

Abstract—The near-bed velocity is a key physical parameter in hydrological, ecological and geomorphological studies. Considering climate change, measurement methods capable of providing continuous observations are needed to assess and predict the effects of increasing uncertainty. Therefore, a technology gap remains for continuous near-bed measurements. To address this gap, we have developed a multimodal flow measurement device, the hydromast. The hydromast uses a combination of pressure and inertial sensing to measure the near-bed (< 30 cm) velocity. We have previously shown that the device can be used to classify river hydromorphological units. Encouraged by these results, we now show that the same device is also capable of continuously measuring the near-bed velocity in rivers. Ten hydromast prototypes were built and calibrated over the range of 0.01 – 2 m/s in a large-scale laboratory tow tank and validated under natural conditions (0.35 – 1.2 m/s) using 118 turbulent flow measurements in a river. It was found that the streamwise, time-averaged velocity mean estimation error from the hydromast in continuous tests with different methods was 0.095 m/s, as compared with a state-of-the-art acoustic Doppler velocimeter. The contribution of this study is a new method for continuous near-bed velocity measurements, verified with turbulent field data from a river.

Index Terms—Flow velocity, continuous measurement, distributed sensing.

I. INTRODUCTION

THE measurement of flow velocity is one of the most important and commonly collected field metrics for hydrological studies [1], sediment transport investigations [2]–[4] and the determination of aquatic habitats [5], [6] in rivers, estuaries and coastal waters. Established field measurement devices in the geosciences rely on flow velocity measurement using propellers and acoustic Doppler velocimetry (ADV). A significant drawback of these devices is that they are best suited for measurements in the water column, as they perform poorly near surfaces due to acoustic backscatter. The majority of remote sensing methods are limited to producing estimates of the surface velocity [7]–[9]. However, the near-bed velocity is a key metric used in sediment transport and river habitat studies [10], [11]. Methods are needed which can provide continuous, distributed data of the near-bed velocity, especially to improve the accuracy of remote sensing estimates.

Motivated by the changing hydrological conditions imposed by climate change and the need for near-bed continuous measurements, a new method for in-situ observations of flow velocity is proposed. A bimodal, redundant flow sensing device, the hydromast was constructed. The bimodal device combines pressure and inertial sensors to improve redundancy. The bimodal design has already been successfully applied to automatically classify river hydromorphology [12]. In this work, we develop new methods for near-bed velocity measurement. The hydromasts were calibrated in a laboratory tow tank and the measurement methods are validated via field experiments in a river. The total and differential pressure are obtained alongside the inertial response of an elastically damped stem. The stem frequency is determined by vortex-induced vibration (VIV). We show that the VIV is directly proportional to the freestream flow velocity. Four different velocity estimation methods are compared; the stem mean power spectral density, the stem dominant frequency in the streamwise and lateral axes, as well as the differential pressure. The results of our investigation show that the device is capable of robustly estimating the time-averaged velocity in real-world field conditions with average accuracy of 0.095m/s, when compared to a Vectrino Profiler.

The primary contributions of this work are:

1) A new device and method for near-bed velocity estimation suitable for continuous measurement with accuracy similar to that of a commercially-available ADV in the streamwise direction.

2) Improved fault tolerance of field velocity measurements. This is achieved via redundant velocity estimates from each device, based on the complimentary pressure and inertial sensing modalities.

The organization of this work is as follows; Section II introduces the device and methods to estimate near-bed velocities using the hydromast. Section III provides the results of the laboratory and field studies. Section IV critically evaluates the hydromast performance considering existing technologies. Section V concludes the work by discussing the strengths, weaknesses and potential applications of the hydromast for continuous, near-bed velocity estimation in shallow waters.

II. METHODS

The calibration of the hydromasts' response to flow was performed in an indoor tow tank and validated in the field (Figure 1). The tow tank allowed testing multiple hydromast prototypes in a controlled environment under
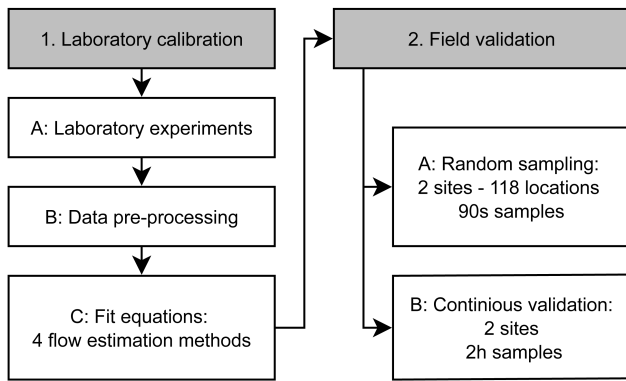
Fig. 1. Workflow showing the calibration and validation procedure used in this study for near-bed velocity estimation using a hydromast.

Fig. 2. Hydromast internal design and the axis of the vibrating IMU.

steady flow conditions. Semi-empirical fit equations between the hydromast sensor readings and the time-averaged velocity were found by mounting the hydromasts to the carriage and propelling them through still water with velocities ranging up to 2 m/s. The results of these equations provided redundant flow estimation methods. Afterwards, 118 short-term (90s) and 2 long-term (1hr) in-situ turbulent velocity measurements were taken in a river and the flow estimation methods were applied. The results were used to validate the device's performance against a state-of-the art ADV.

The following subsections provide detailed information on the two stages.

A. Hydromast Design

The hydromast is inspired by the biological lateral lines, which are the mechanoreceptive flow sensing organs of fish. Specifically, it is an upscaled version of the neuromast, and consists of a vibrating stem elastically fixed to a pressure sensitive body. The bulk flow velocity drives the stem vibration, as the random forcing due to turbulence tends to cancel itself out [13]. Furthermore, the stem integrates hydrodynamic interactions over its height. The stem motion is recorded with a micromechanical inertial measuring unit (IMU) (BN055, Bosch Sensortech) fixed to its lower end. In a previous laboratory investigation, we have proposed a design which accurately estimated the time-averaged flow speed over the range of 0 to 0.5 m/s [14]. A 100 mm long, 15 mm diameter rigid hollow polyoxymethylene (POM) plastic stem was used in the prototypes. Hollow stems were chosen in order to match the density as close as possible to the surrounding water, minimizing the restoring force caused by buoyancy. The noise introduced by vibrations of the hydromast's body are compensated by adaptive cancellation by subtracting the signals from a second, identical IMU mounted within the base. We have found that a similar approach applied for correction of pressure signals in a fish-shaped lateral line probe provided promising results [15]. In addition, the base IMU also serves as a compass, indicating the absolute orientation of the device relative to magnetic North.

In addition to the inertial-sensing stem, the hydromast also includes three pressure sensors. An absolute pressure sensor records the water depth (MPX5100GP, NXP) and
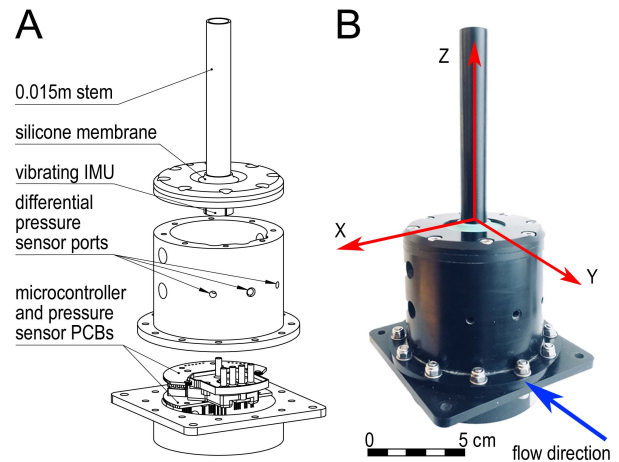
two differential pressure sensors (MPXV7002, NXP) facing into the flow measure the dynamic pressure relative to the stagnation point. The differential sensor module was added in this design, as a similar configuration has proven successful for underwater flow speed estimation [16]. The pressure ports are integrated into the POM casing and are the differential pressure sensors are connected to the housing pressure ports using a custom 3D printed adapter. The complete design of the pressure-inertial hydromast is shown in Figure 2.

B. Working Principles for Velocity Estimation

Fluid-body forces govern the interactions between both the pressure sensors and mast due to vortex induced vibration (VIV). The bimodal design was created to improve fault tolerance by including two distinct velocity estimation methods. In this way, identical flow conditions are perceived in two different, but complementary ways by the sensing body. The pressure sensor readings are instantaneous, whereas the VIV resonator integrates the forcing over temporal and spatial scales smaller than the bulk motion of the sensor, and the stem height, respectively.

The first velocity estimation method introduced in this work is based on the elastically supported rigid stem as a VIV resonator. Our design was motivated by studies on elastically mounted cylinders, which are known to exhibit lock-in phenomen [17]–[19]. Specifically, we tuned our design so that the lightly damped cylinder would oscillate as closely as possible to the natural vortex shedding frequency. Streamwise vibrations of the stem set in when the ratio of vibration f to natural vortex shedding frequency is equal to 4 [13], [20]. Similarly, VIV streamwise motion is exhibited by the cylinder at $f/f_o = 2$. When considering how VIV can be used for flow velocity estimation, an important lock-in phenomenon occurs when the cylinder shedding frequency f_0, is close to resonance f_n, $f_0 = f_n = 1$. In such cases, the shedding becomes controlled by the natural frequency, even if small fluctuations in the flow velocity occur [20]. The VIV modes and their relation to the bulk flow can be visualized through the relation
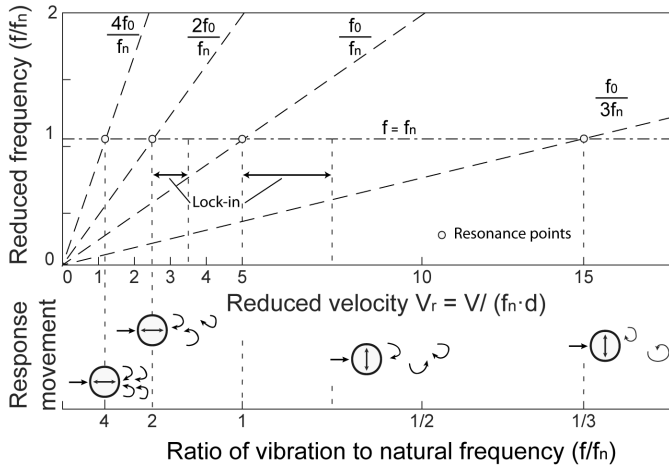
Fig. 3. Schematic response of lightly damped cylinder in crossflow.

between reduced velocity V_r and reduced frequency f/f_n, shown in Figure 3 (adapted from [13]).

The properties of the hydromast were first estimated via a preliminary estimation of the frequency response of an elastically mounted cylinder excited by vortex shedding. The shedding frequencies were calculated based on the Strouhal number (St), where the vortex-shedding frequency fs is given as:

$$f_s = St \frac{U}{D}, \tag{1}$$

where the U is velocity and D is the cylinder diameter. The Strouhal number for fixed cylinders can be approximated as a constant value of 0.2 over a wide range of Reynolds numbers (Re), from 10^3 and 10^5. The vortex street in the far wake (shown in Figure 3) has a Strouhal frequency f_s, and within the lock-in ranges, the observed frequencies deviate very little from the theoretical estimates [13]. The frequency of the stem's linear acceleration in the streamwise direction is therefore close to the theoretical vortex shedding frequency. At the same time, the vortex induced vibration perpendicular to the flow is twice the streamwise frequency [13]. The vortex shedding frequency increases linearly with the freestream flow velocity, allowing for the use of the dominant frequencies of the perpendicular (major) and streamwise (minor) vortex-induced vibrations to estimate the streamwise flow velocity. Taking this into account, we propose the following linear model relating the hydromast stem's vortex shedding frequency f_s with the flow speed, based on the measured dominant frequencies of the linear acceleration sensor readings:

$$V_{fx} = ax \cdot f_x + cx, \tag{2}$$
$$V_{fy} = ay \cdot f_y + cy, \tag{3}$$

where ax, ay and cx, cy are the calibration constants, and f_x and f_y are the dominant frequencies of the linear acceleration of the stem in the streamwise and perpendicular directions, respectively.

In our previous work, we showed that the time-averaged velocity can also be estimated using the mean frequency spectra amplitude after taking the Fast Fourier Transform (FFT) of the stem vibrations [14]. We also applied this estimation

method in the current study, based on the relation of the mean power spectral density PSD of the linear acceleration magnitude to the flow speed using a power function:

$$V_{PSD} = k \cdot mPSD^b + l, \tag{4}$$

where k, l and b are the calibration constants and $mPSD$ the recorded mean PSD of the stem.

Complimentary to, but independent of the hydromast stem, are redundant velocity estimates derived from the collocated synchronized pressure sensors. The differential pressure (DP) sensors were calibrated against the oncoming flow speed based on the Fechheimer-Pitot concept. This method is discussed in our previous works on pressure-based underwater velocity estimation for autonomous vehicles [16]. The working principle of a Fechheimer-Pitot is that for a vertically-oriented circular cylinder facing into a flow with freestream velocity U_∞ the velocity U_θ acting on an surface element at angle θ is given by:

$$U_\infty = \sqrt{\frac{2\Delta p}{\rho 4 sin^2 \theta}}, \tag{5}$$

Assuming a constant water density, and that the sensing body and flow direction are fixed, the equation can be simplified by introducing the constant α:

$$\alpha = \frac{1}{4\rho \sin^2 \theta}, \tag{6}$$

The freestream flow velocity is then estimated by taking the arithmetic mean of the two differential sensor readings using the Pitot-static relation:

$$V_{DP} = U_\infty = \sqrt[4]{\alpha(\Delta P_1^2 + \Delta P_2^2)}, \tag{7}$$

where ΔP is the differential pressure sensor reading in mV and α is the calibration constant. It has been shown that the relation can provide a highly accurate instantaneous flow speed estimation, including yaw angles up to $\pm 45°$ [3].

Calibration constants to the four proposed methods, V_{fx}, V_{fy}, V_{PSD} and V_{DP} were found experimentally and these procedures are described in the following section.

C. Laboratory Calibration

1) Laboratory Calibration Experimental Setup: The laboratory calibration was performed in an indoor tow tank with a total length 60 m, and an effective measurement distance of 46 m (including acceleration/deceleration) located at the TalTech Small Craft Competence Centre (SCC) in Kuressaare, Estonia. The still water depth was 3 m, and the tank has a constant cross-sectional width of 5 m. The towing carriage allows testing at speeds from 0.01 to 5.5 m/s.

To facilitate a comparison between prototypes, an array of five identical hydromasts was fixed to the carriage and calibrated as an ensemble. Each hydromast was fixed to the carriage using an aluminum frame (45x45 UL profiles, MiniTec Framing Systems LLC) oriented perpendicular to the direction of motion. Incremental steps in carriage speeds were used to calibrate the hydromasts (0.02, 0.04, 0.07, 0.12, 0.19, 0.27, 0.37, 0.50, 0.66, 0.84, 1.07, 1.33, 1.63 and 2 m/s).
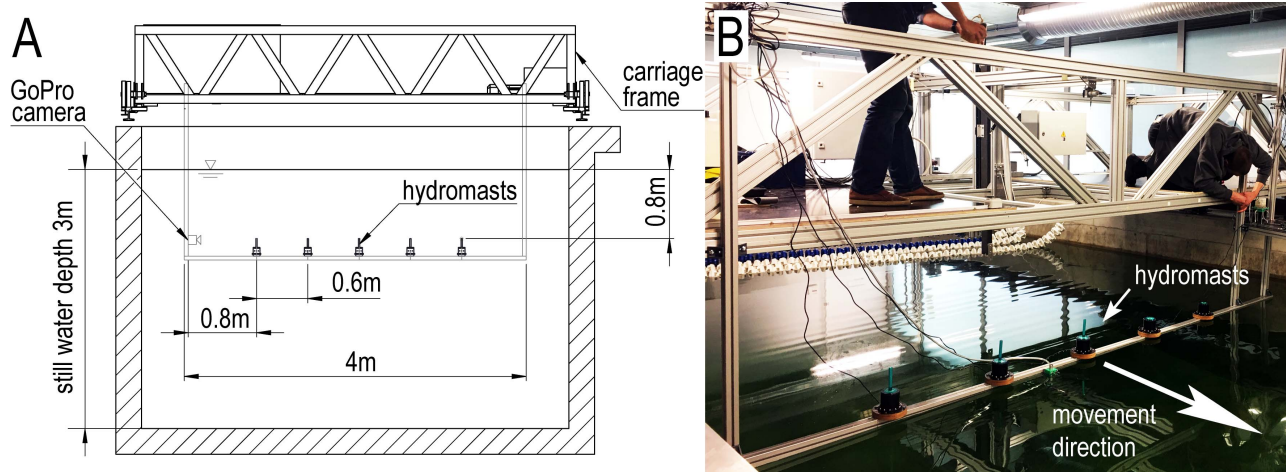
Fig. 4. Tow tank dimension and the positioning of the hydromasts on the moving frame.

At lower speeds (up to 0.12 m/s) the carriage was actuated for a total duration of 5 minutes. At higher speeds, the data were logged until the carriage reached the end of the tank. The experiments were repeated twice at lower speeds and three times at higher speeds. For each repetition, the carriage speed was recorded with an accuracy of 0.01 m/s (Incremental Encoders: 8.5000.8354.5000, Fritz Kübler GmbH). The top of the hydromast stems were submerged 0.8m from the still water surface. A GoPro Hero 3 (GoPro Inc., USA) camera was fixed on the side of the frame for subsequent analysis of the hydromast stem movements. The experimental setup is shown in Figure 4.

The five hydromasts were connected to a laptop (Lenovo T440, Intel Core i5-4300U CPU) through two USB hubs (7-Port USB 2.0 Hub DUB-H7, D-Link). The data logging was performed with TeraTerm software (Tera Term Project). The hydromasts were synchronized by sending a start command to the standby devices before each experiment, and subsequently powered off after each run. The output of each hydromast consisted of 25 columns: the timestamp in ms; absolute and differential pressure sensors outputs in mV; quaternions, dynamic and gravitational accelerations in mg from the two IMUs; and the temperature of the internal stationary IMU.

2) Data Pre-Processing: The data from the laboratory experiments were first visually inspected for faults using the five stem IMUs. This was done by plotting the dynamic acceleration and angular time series. Since the mean values of the carriage velocity were used as the ground truth for the velocity calibration, no synchronization was required between the carriage speed recordings and the hydromast sensors. All time series were truncated to the period over which the carriage was moving at a constant velocity. As the experimental runs duration was shortening with the increase in flow velocity, 15,000 samples of each dataset were used.

The stem and differential pressure sensor data were pre-processed before comparison with the time-average carriage. First, readings from the body-mounted hydromast IMU were used to adaptively filter external vibrations experienced by the stem. External vibrations were caused by the experimental setup, especially due to the frame as it was dragged through the tank. The pre-processed data were then fitted to the carriage speeds using the data processing workflow presented in Figure 1. All signal processing was performed using MATLAB 2015a (MathWorks Inc., USA).

D. River Field Measurements

After the fit equations were tested using the hydromast stem and pressure sensor data to the carriage speed, validation experiments were conducted in the field. The objective was to compare the hydromast flow velocity estimates with a commercial ADV under real-world conditions in a shallow river, using 118 single point samples (90s) and 2 continuous measurements (1hr). A factory-calibrated acoustic Doppler profiler (Vectrino Profiler, Nortek AS, Rud, Norway) was used which is capable of measuring the three-dimensional flow velocity over a vertical profiling range of 30 mm. The Vectrino Profiler was chosen because it has been used successfully in high-precision open channel flow experiments, both in the laboratory and in the field to measure near-bed flows [21]–[24].

A field measurement setup with the Vectrino profiler and a single hydromast was assembled, and is shown in Figure 4. The probe of the Vectrino profiler was fixed 100 mm from the stem in horizontal plane and 40mm from the top of the stem. The data was logged both with ADV and with hydromast for 90 seconds at single point sampling for 1 hour in the continuous sampling scenario. The sampling rate of the hydromast was 100Hz and the ADV data was logged at 15Hz. The ADV data recording was remotely activated using an Intel Compute Stick (Intel Corporation). The hydromast data was recorded to a custom data logger based on a Raspberry Pi 2 (The Raspberry Pi Foundation). The ADV and hydromast logging were synchronized to evaluate the prediction accuracy and to assess the potential influence of flow turbulence on the hydromast. As in the laboratory experiments, the differential pressure offsets were recorded prior to field measurements and included in the differential pressure-based velocity estimation.
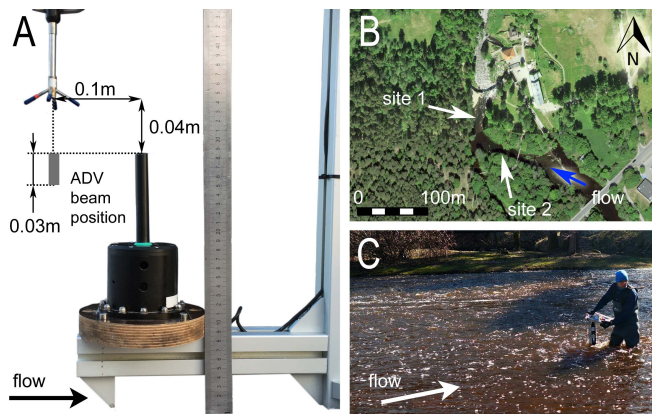
Fig. 5. Field setup for hydromast velocity validation using a vectrino profiler. A - Side view of the position of the ADV/hydromast position. B - Site locations on Keila river. C. Sampling at site no 2.

Fig. 6. Video stills from stem angles at different speeds and modes. A - 0.33 m/s. B - 0.84 m/s. C - 1.63 m/s.

The validation tests were conducted at the Keila River (latitude: 59.395017 N, longitude: 24.29442 E; closest address: Posti 1, Keila-Joa, 76701 Harju county, Estonia). Field data was collected at two different sites, immediately upstream of the Keila Waterfall as they had different substrate and flow characteristics, allowing for the inclusion of natural variability of in situ flow conditions. The first site had a flat, smooth limestone bed and calm water surface, whereas the upstream site had a rocky bottom and highly undulating water surface. At both sites, the river had a bankfull width of 27 m and a discharge approximately of 16.5 m/s^3. A total of 118 randomly-chosen locations were measured.

The raw ADV signal was recursively despiked 20 times using the phase-space method after Goring and Nikora [25]. The despiked signal was then used for calculating the time-averaged flow velocity and the RMS value of the zero-mean fluctuations (turbulence intensity, TI) at each measurement point.

III. RESULTS

A. Laboratory Tow Tank

The laboratory experiments were carried out to confirm the working principles of the inertial and differential pressure sensors, and to generate the fit equations used in each of the velocity estimation methods. In total, four different estimation methods for the near-bed flow velocity were compared:

1. Dominant stem frequency, linear acceleration in the streamwise direction;
2. Dominant stem frequency, linear acceleration perpendicular to the streamwise flow direction;
3. Mean power spectral density amplitude from the stem acceleration magnitude;
4. Differential pressure Pitot-equation regression.

The hydromast tow tank experiments aligned well with the theory, as shown in Figure 6. A total of three modes were found: mode 1 corresponded to no vibrations of stems up to velocities of 0.5 m/s. Mode 2 corresponded to VIV covering a range of velocities from 0.5 m/s to 1.07 m/s. Mode 3 began at 1.3 m/s and was characterized by dominant flow-induced
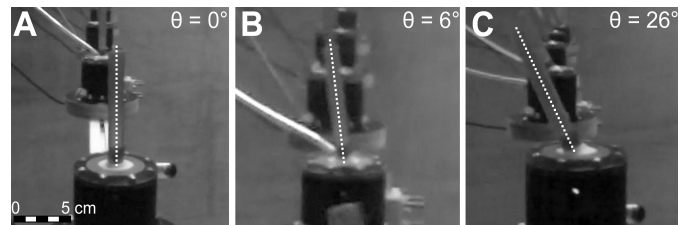
forcing of the stem, causing the stem to remain at a fixed angle of response. The calibration experiments show that both the streamwise and perpendicular linear acceleration of the stem are proportional to the freestream flow velocity. Crossflow vibrations emerge when the stem vibration frequency f ratio to natural frequency is $f/f_n = 1$. Natural frequency f_n of the masts in water was found to be 6 Hz. At f/f_n ratios 1 to 1/3 the stem vibrations grow linearly with adjusted R^2 values of 0.99 for stream wise movements (y-axis) and 0.97 for the perpendicular movements (x-axis). In this range, the stem oscillates in a figure of eight pattern; the higher frequency in the freestream flow direction, and one half the frequency perpendicular to the flow (Figure 7). Furthermore, two modes are distinguishable, one for flow velocities ranging from 0.02 - 0.35 m/s and the second from1.3 – 2.0 m/s, corresponding to the device's target range. Due to the vibrations introduced by the carriage motion at low velocities, the recorded vibrations between f/f_n ratios of 4 and 2 were clearly not correlated to the actual movements of the stem and were excluded from the calibration.

Video recordings of the calibration experiments verified the results showing no onset of stem movement below 0.5 m/s, and the stem position remained stationary for flow velocities higher than 1.3 m/s (Figure 6).

The third velocity estimation method used the mean PSD spectrum amplitude to estimate flow velocity. The mean PSD was calculated from the x-and y-axis linear acceleration component's magnitude with base vibrations removed. The mean PSD values showed two distinguishable modes of all of the hydromasts' stems. The response of the masts' PSD mean values to flow speed up to 1.1 m/s followed a polynomial relation. No clear relation between flow velocity and the mast's PSD mean values were found above velocities 1.3 m/s.

The fourth method for velocity estimation made use of the Fechheimer-Pitot concept based on the differential pressure sensors (Figure 8). In contrast to the velocity estimation methods using the stem, the differential pressure sensors covered the full velocity range of the calibration test tank.

The fit values of the 4 models are given in Table 1. Considering that all four methods provide redundant velocity data, the hydromast fulfilled the second objective of this study which was to provide fault-tolerant near-bed velocity estimates. Comparing the four methods, it was found that the new method proposed in this work based on VIV using the dominant frequencies had the best overall performance. The second best performance was from the differential
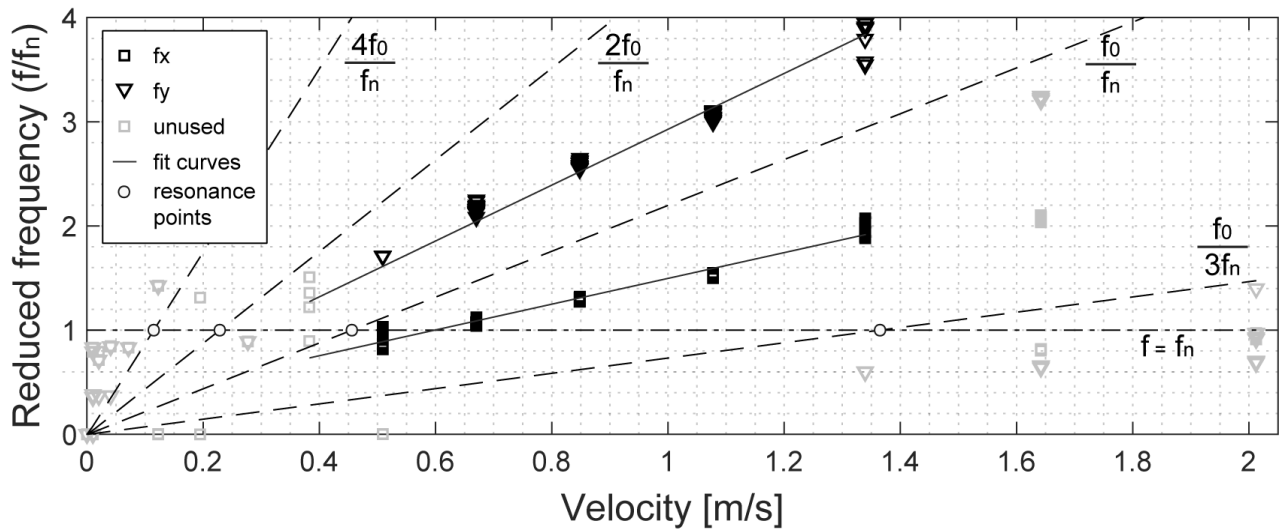
Fig. 7. Hydromast stem x- and y-axis vibrations fit to flow speed up to 2 m/s.
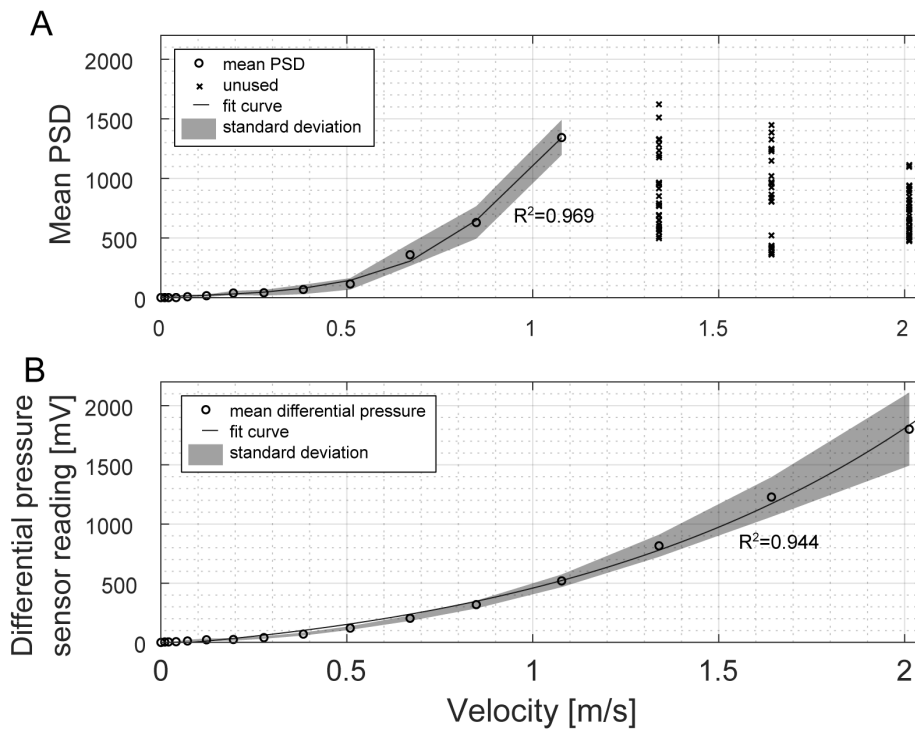
Fig. 8. A - Mean PSD values of the stem. B - Right/left differential pressure sensor mean outputs up to 2 m/s.

pressure estimates, and our previous estimation method using the mean stem linear acceleration PSD had the lowest overall performance.

B. Validation

Three hydromasts were used for the field validation experiments in the single point sampling scenario. Based on a comparison with ADV measurements velocities varied between 0.35 m/s to 1.5 m/s. A total of 118 measurement points were taken from the field. The results of the four different velocity estimation methods are plotted against the time-averaged ADV velocity V_{ADV} in Figure 9. The turbulence intensity was plotted in greyscale. Based on the field data, turbulence was not found to have a systematic impact on any of the velocity estimation methods.

Overall, the estimates using the dominant frequency method perform poorly for velocities below 0.5 m/s. The round mean absolute error (RMSE) taking the ADV measurements as ground truth above velocities 0.5 m/s was 0.11 m/s for x-axis and 0.09 m/s for y-axis As seen in Figure 9. V_{fx} and V_{fy} perform well when compared with V_{ADV} (R2 of 0.932 and 0.941 for V_{fx} and V_{fy} respectively).
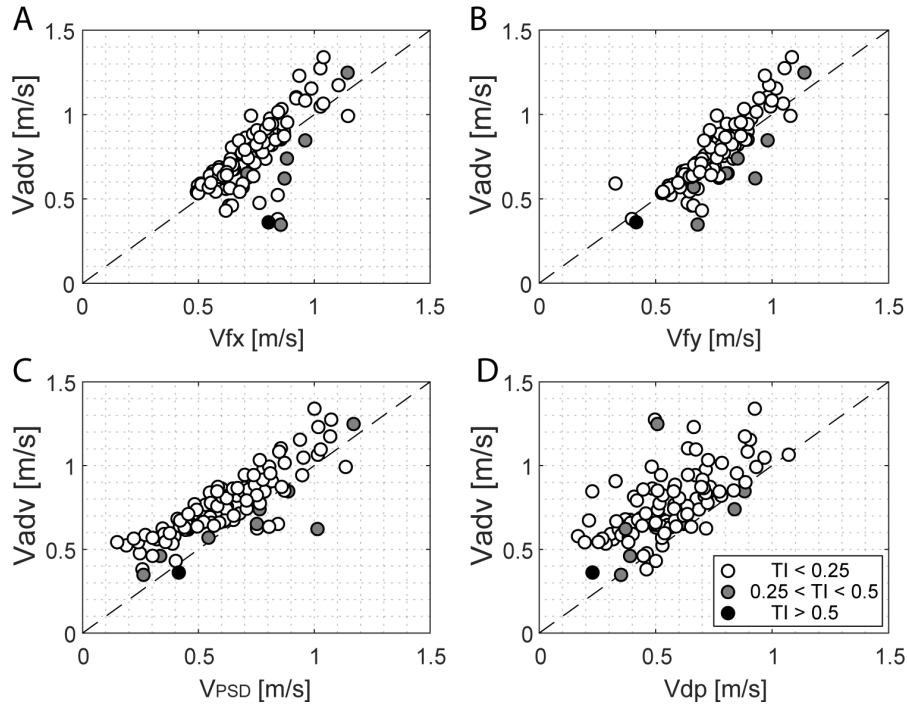
Fig. 9. Flow estimation with different methods with TI color marked. A-estimates with the mast dominant frequency perpendicular to the flow. B-estimates with the mast dominant frequency along the flow. C-estimates with the mean PSD values. D-estimates with differential pressure.

TABLE I

FIT VALUES OF THE 4 VELOCITY ESTIMATION MODELS

	mean PSD fit (0 to 1.1 m/s)	dominant frequency x-axis (0.5 to 1.3 m/s)	dominant frequency y-axis (0.5 to 1.3 m/s)	differential pressure (0 to 2 m/s)
Adjusted R^2	0.969	0.971	0.986	0.995
RMSE	0.068	0.051	0.038	0.049
SSE	1.066	0.295	0.145	0.864

The V_{PSD} RMSE values were higher, reaching an error of up to 0.19 m/s. Errors were calculated for velocities up to 1.1 m/s, where the response of the V_{PSD} was cut off, see Figure 8. In general, the V_{PSD} values tended to underestimate the velocities, but their overall performance still exhibited a strong correlation with the V_{ADV} readings (R2 of 0.854). It is visible from Figure 9 that the VPSD flow estimates closely track the ADV velocity values, but that 90% of them have a negative offset.

The differential pressure module velocities were found to have to systematically underestimate the ADV measurements. Overall. the correlation coefficient between V_{ADV} and V_{DP} module was the lowest of the four methods tested at 0.670. The RMSE of the V_{DP} was 0.26 m/s of the DP fit functions.

In the continuous sampling scenario, data was recorded for 1 hour at two sites. The round mean square error from the ensemble of all four methods was 0.095 m/s considering both sites. The results of the continuous river experiments are provided in Table 2.

IV. DISCUSSION

In general, the results of this study show promising relations between the flow velocity estimates for all four of the hydromast estimation methods. However, there remain some considerations and limitations which should be further discussed.

A drawback of the tow tank calibration was that gantry frame's vibrations, which affected the PSD mean velocity estimation performance. This resulted in V_{PSD} underestimating some 90% of the velocity data. To use the PSD mean value method for velocity estimation, the hydromasts should use fit equations from similar physical conditions as those found in the field. This will likely reduce the calibration bias significantly. Another consideration when using the hydromast PSD mean values for velocity estimates is that periodic forcing such as waves will increase the velocity estimate error by shifting the PSD distribution.

Similarly, vibrations introduced during the gantry movement at low speeds did not allow us to study the full span of low velocities from 0 to 0.25 m/s. Theoretically, it should be possible to pick up lower velocities, where the stem movement is dominated by streamwise vortices and vibrations remain relatively small. It would be beneficial to use an experimental setup with the hydromasts firmly fixed to the bed, and with the possibility to alternate the flow velocity.

The river field validation showed some deviation from the ADV measurements although the differential pressure sensor model calibration curves followed the modified Pitot equation with high R^2 values. The low correlation to the field measurements of the ADV can be related to pressure fluctuations of the water surface and higher turbulence within the flow at the

TABLE II
TWO 1 H EXPERIMENTAL RUNS ON CALM AND TURBULENT FLOWS (UNITS m/s)

Site	VADV	V_{fx}	V_{fy}	V_{PSD}	V_{DP}	RMSE V_{fx}	RMSE V_{fy}	RMSE V_{PSD}	RMSE V_{DP}
1- calm	0.644	0.625	0.680	0.504	0.637	0.019	0.038	0.141	0.012
2 - rough	0.973	0.875	0.890	0.885	0.709	0.104	0.091	0.093	0.265

rocky site. The turbulence affecting the pressure difference on the cylindrical body of the hydromast could come from the vertical surface motion of the water surface as the low sections of the rivers was used. At some of the measurement locations, the river was only 0.3 m deep. Also, local pressure fluctuation and vortices formed from rocks and close to the rocky surface could be another cause of pressure changes in the field. In order to take into account, the pressure changes due to the turbulence of the flow and in the close vicinity of the bottom may require additional correction factors.

The field validation experiments showed that the estimation errors tend to decrease as the sampling time increases. This was observed across all four methods, as described section III-B. The improved results can be explained quite simply: a larger number of samples reduces the effect of turbulent fluctuations on the velocity estimate. The errors associated with the turbulent flows were generally found to be higher. Only the PSD model's error was reduced. However, we believe this was not a feature of the measurement or data processing method, but may be attributed to the turbulent flow environment being closer to the background noise of the tow tank setup. Both streamwise and perpendicular stem vibration models showed that a small decrease in estimation accuracy may occur for long-term turbulent flows. This too, may be caused not by a fundamental feature of the device, by rather by diurnal changes in the time-average velocity itself.

We show that hydromast can provide a new way for the bimodal, redundant measurement of near-bed velocity in nature. The small size and low price (estimated as roughly 1/10th of a commercial ADV) of the hydromast could allow distributed seasonal studies in a variety of shallow water applications. Such measurements using ADVs is unlikely to occur due to cost considerations alone. We are optimistic that the scalability of the hydromasts may open up new application fields; distributed sensing for model calibration of remote sensing data, nutrient and waste movement, sediment transport studies in rivers or along the coastline and provide real-time monitoring of seasonal changes in near-bed river velocities during extreme events such as droughts and flooding.

V. CONCLUSIONS

In this study we introduced a new method for estimating near-bed velocity using a bioinspired, bimodal redundant measuring device, the hydromast. A benefit of using the hydromast is that the dominant frequency velocity estimation approach can work well in a noisy environment. This is because background fluctuations at a physical scale smaller than the stem's length act as a stochastic forcing, effectively cancelling each other out. This feature is useful at locations with high relative background turbulence. Although the fluid-body interactions between the stem and a fully turbulent flow field are complex, the hydromast stem geometry and membrane stiffness largely determine its sensitivity and range. In contrast to existing sensing methods, the hydromast can be customized to mechanically filter specific flow conditions.

The device is designed based on first principles, and its performance was validated using real-world field data in a turbulent river. Future work will focus on tuning hydromasts to a wider range of flow conditions, including lower and higher ranges of flow velocities. In addition, long-term tests of several months in freshwater and saltwater environments are planned to establish operational issues associated with seasonal change, long-distance cabled data transfer and biofouling.

REFERENCES

[1] S. L. Dingman, *Physical Hydrology*, 3rd ed. Waveland, MS, USA: Waveland Press, 2015.

[2] K. F. E. Betteridge, J. J. Williams, P. D. Thorne, and P. S. Bell, "Acoustic instrumentation for measuring near-bed sediment processes and hydrodynamics," *J. Exp. Mar. Bio. Ecol.*, vols. 285–286, pp. 105–118, Feb. 2003.

[3] R. Kostaschuk, J. Best, P. Villard, J. Peakall, and M. Franklin, "Measuring flow velocity and sediment transport with an acoustic Doppler current profiler," *Geomorphology*, vol. 68, nos. 1–2, pp. 25–37, May 2005.

[4] B. Elfrink and T. Baldock, "Hydrodynamics and sediment transport in the swash zone: A review and perspectives," *Coast. Eng.*, vol. 45, nos. 3–4, pp. 149–167, May 2002.

[5] F. D. Shields and J. R. Rigby, "River habitat quality from river velocities measured using Acoustic Doppler current profiler," *Environ. Manage.*, vol. 36, no. 4, pp. 565–575, Oct. 2005.

[6] L. A. Levin *et al.*, "The function of marine critical transition zones and the importance of sediment biodiversity," *Ecosystems*, vol. 4, no. 5, pp. 430–451, Aug. 2001.

[7] W. J. Plant, W. C. Keller, and K. Hayes, "Measurement of river surface currents with coherent microwave systems," *IEEE Trans. Geosci. Remote Sens.*, vol. 43, no. 6, pp. 1242–1257, Jun. 2005.

[8] R. P. Mied *et al.*, "Airborne remote sensing of surface velocities in a tidal river," *IEEE Trans. Geosci. Remote Sens.*, vol. 56, no. 8, pp. 4559–4567, Aug. 2018.

[9] A. Hauet, J.-D. Creutin, and P. Belleudy, "Sensitivity study of large-scale particle image velocimetry measurement of river discharge using numerical simulation," *J. Hydrol.*, vol. 349, nos. 1–2, pp. 178–190, Jan. 2008.

[10] A. Recking, "Theoretical development on the effects of changing flow hydraulics on incipient bed load motion," *Water Resour. Res.*, vol. 45, no. 4, pp. 1–16, Apr. 2009.

[11] B. N. Bockelmann, E. K. Fenrich, B. Lin, and R. A. Falconer, "Development of an ecohydraulics model for stream and river restoration," *Ecol. Eng.*, vol. 22, nos. 4–5, pp. 227–235, Jul. 2004.

[12] A. Ristolainen, K. Kalev, J. A. Tuhtan, A. Kuusik, and M. Kruusmaa, "Hydromorphological classification using synchronous pressure and inertial sensing," *IEEE Trans. Geosci. Remote Sens.*, vol. 62, no. 11, pp. 1–11, Nov. 2018.

[13] E. Naudascher and D. Rockwell, *Flow-Induced Vibrations: An Engineering Guide Dover Civil and Mechanical Engineering*. New York, NY, USA: Dover, 2005.

[14] A. Ristolainen, J. A. Tuhtan, A. Kuusik, and M. Kruusmaa, "Hydromast: A bioinspired flow sensor with accelerometers," in *Biomimetic and Biohybrid Systems*, vol. 9793, N. F. Lepora, A. Mura, H. G. Krapp, P. F. M. J. Verschure, and T. J. Prescott, Eds. Berlin, Germany: Springer, 2016, pp. 510–517.

[15] J. A. Tuhtan *et al.*, "Design and application of a fish-shaped lateral line probe for flow measurement," *Rev. Sci. Instrum.*, vol. 87, no. 4, Apr. 2016, Art. no. 045110.

[16] J. F. Fuentes-Pérez, K. Kalev, J. A. Tuhtan, and M. Kruusmaa, "Underwater vehicle speedometry using differential pressure sensors: Preliminary results," in *Proc. IEEE/OES Auto. Underwater Vehicles (AUV)*, Nov. 2016, pp. 156–160.

[17] S. Mittal and V. Kumar, "Flow-induced vibrations of a light circular cylinder at Reynolds numbers 103 to 104," *J. Sound Vib.*, vol. 245, no. 5, pp. 923–946, Aug. 2001.

[18] C. H. K. Williamson and R. Govardhan, "A brief review of recent results in vortex-induced vibrations," *J. Wind Eng. Ind. Aerodyn.*, vol. 96, nos. 6–7, pp. 713–735, Jun./Jul. 2008.

[19] T. Sarpkaya, "A critical review of the intrinsic nature of vortex-induced vibrations," *J. Fluids Struct.*, vol. 19, no. 4, pp. 389–447, May 2004.

[20] G. Morgenthal, *Fluid Structure Interaction in Bluff-Body Aerodynamics and Long-Span Bridge Design: Phenomena and Methods*. Cambridge, U.K.: Univ. of Cambridge, Department of Engineering, 2000.

[21] X. Leng and H. Chanson, "Integral turbulent scales in unsteady rapidly varied open channel flows," *Exp. Therm. Fluid Sci.*, vol. 81, pp. 382–395, Feb. 2017.

[22] A. Brand and C. Noss, "High-resolution flow characterization close to the sediment-water interface in a run of the river reservoir," *Water Resour. Res.*, vol. 53, no. 5, pp. 4286–4302, May 2017.

[23] M. Peters, S. P. Clark, K. Dow, J. Malenchak, and D. Danielson, "Flow characteristics beneath a simulated partial ice cover: Effects of ice and bed roughness," *J. Cold Reg. Eng.*, vol. 32, no. 1, Mar. 2018, Art. no. 04017017.

[24] R. E. Thomas, L. Schindfessel, S. J. McLelland, S. Creëlle, and T. De Mulder, "Bias in mean velocities and noise in variances and covariances measured using a multistatic acoustic profiler: The Nortek Vectrino Profiler," *Meas. Sci. Technol.*, vol. 28, no. 7, Jul. 2017, Art. no. 075302.

[25] D. G. Goring and V. I. Nikora, "Despiking acoustic Doppler velocimeter data," *J. Hydraul. Eng.*, vol. 128, no. 1, pp. 117–126, Jan. 2002.

Asko Ristolainen received the B.Sc. and M.Sc. degrees in mechatronics and the Ph.D. degree in information and communication technology from the Tallinn University of Technology, Tallinn, Estonia, in 2008, 2010, and 2015, respectively.

He is currently a Researcher with the Centre for Biorobotics, School of Information Technologies, Tallinn University of Technology, where he is involved in the Lakhsmi Project. His research interests include environmental sensing, flow sensor design, and mechanics.

Jeffrey A. Tuhtan received the B.Sc. degree in civil engineering from California Polytechnic University, San Luis Obispo, CA, USA, in 2004, and the M.Sc. degree in water resources engineering and management and the Dr.Eng. degree from the University of Stuttgart, Germany, in 2007 and 2011, respectively.

He is currently with the Centre for Biorobotics, Tallinn University of Technology, where he leads the Environmental Sensing and Intelligence Group. His current research interests include environmental intelligence and bio-inspired underwater sensing.

Maarja Kruusmaa received the Dipl.Eng. degree in computer engineering from the Tallinn University of Technology, Estonia, in 1994, and the Ph.D. degree in computer engineering from the Chalmers University of Technology, Gothenburg, Sweden, in 2002.

She is currently the Head of the Centre for Biorobotics, Tallinn University of Technology. During the past years, she was involved in flow sensing underwater robots, bio-inspired robot locomotion, and experimental fluid dynamics. Her research mainly focuses on bio-inspired underwater robotics.